

Novel Hsp90 inhibitor NVP-AUY922 radiosensitizes prostate cancer cells

Nishant Gandhi,^{1,†} Aaron T. Wild,^{1,†} Sivarajan T. Chettiar,¹ Khaled Aziz,¹ Yoshinori Kato,^{2,3} Rajendra P. Gajula,¹ Russell D. Williams,¹ Jessica A. Cades,^{1,2,4} Anvesh Annadanam,¹ Danny Song,^{1,2,5} Yonggang Zhang,¹ Russell K. Hales,¹ Joseph M. Herman,¹ Elwood Armour,¹ Theodore L. DeWeese,^{1,2,5} Edward M. Schaeffer^{2,5} and Phuoc T. Tran^{1,2,*}

¹Department of Radiation Oncology & Molecular Radiation Sciences; Sidney Kimmel Comprehensive Cancer Center; Johns Hopkins University School of Medicine; Baltimore, MD USA; ²Department of Oncology; Sidney Kimmel Comprehensive Cancer Center; Johns Hopkins University School of Medicine; Baltimore, MD USA; ³Russell H. Morgan Department of Radiology and Radiological Sciences; Division of Cancer Imaging Research; Johns Hopkins University School of Medicine; Baltimore, MD USA; ⁴Department of Pharmacology and Molecular Sciences; Johns Hopkins University School of Medicine; Baltimore, MD USA; ⁵Department of Urology; Johns Hopkins University School of Medicine; Baltimore, MD USA

[†]These authors contributed equally to this work.

Keywords: prostate cancer, Hsp90, NVP-AUY922, radiosensitizer, DNA damage response

Outcomes for poor-risk localized prostate cancers treated with radiation are still insufficient. Targeting the “non-oncogene” addiction or stress response machinery is an appealing strategy for cancer therapeutics. Heat-shock-protein-90 (Hsp90), an integral member of this machinery, is a molecular chaperone required for energy-driven stabilization and selective degradation of misfolded “client” proteins, that is commonly overexpressed in tumor cells. Hsp90 client proteins include critical components of pathways implicated in prostate cancer cell survival and radioresistance, such as androgen receptor signaling and the PI3K-Akt-mTOR pathway. We examined the effects of a novel non-geldanamycin Hsp90 inhibitor, AUY922, combined with radiation (RT) on two prostate cancer cell lines, Myc-CaP and PC3, using in vitro assays for clonogenic survival, apoptosis, cell cycle distribution, γ -H2AX foci kinetics and client protein expression in pathways important for prostate cancer survival and radioresistance. We then evaluated tumor growth delay and effects of the combined treatment (RT-AUY922) on the PI3K-Akt-mTOR and AR pathways in a hind-flank tumor graft model. We observed that AUY922 caused supra-additive radiosensitization in both cell lines at low nanomolar doses with enhancement ratios between 1.4–1.7 ($p < 0.01$). RT-AUY922 increased apoptotic cell death compared with either therapy alone, induced G₂-M arrest and produced marked changes in client protein expression. These results were confirmed in vivo, where RT-AUY922 combination therapy produced supra-additive tumor growth delay compared with either therapy by itself in Myc-CaP and PC3 tumor grafts (both $p < 0.0001$). Our data suggest that combined RT-AUY922 therapy exhibits promising activity against prostate cancer cells, which should be investigated in clinical studies.

Introduction

Prostate cancer remains the most common non-cutaneous cancer in men and the second leading cause of cancer mortality among men in the United States.¹ Radiation therapy is a well-established standard treatment option for localized and locally advanced prostate cancer with high biochemical control rates for low-risk localized disease.^{2,3} However, radiation efficacy for intermediate-risk localized and less favorable disease requires improvement. Subsets of these poor prognosis patients treated with definitive radiation therapy will experience biochemical failure in greater than 30% of cases.^{4–6} Efforts to improve the efficacy of radiation therapy by escalating the physical dose of radiation administered have reached a maximum secondary to dose-limiting rectal and genitourinary toxicity. Another approach to augment the efficacy of radiation therapy without simultaneously increasing the risk to

normal tissues is biologic escalation of the radiation dose to the tumor through the use of tumor-specific radiosensitizing agents.

Targeting the non-oncogene addiction or stress response machinery is an intriguing option for cancer therapeutics. Tumor cells are subjected to high levels of proteotoxic stress caused by chronic and acute hypoxia, increased levels of DNA damage, high levels of reactive oxygen species and protein complex imbalances due to aneuploidy.⁷ Survival under these conditions is afforded by the aid of efficient cellular stress response machinery, such as heat shock proteins (Hsp). Hsp90 is a ubiquitous molecular chaperone, found to be overexpressed in a variety of cancers, including prostate cancer. Hsp90 stabilizes misfolded proteins through an energy driven process, preventing protein aggregation while selectively directing others towards degradation.⁸ Among its client proteins are transcription factors, cell cycle regulators, signaling kinases, mediators of apoptosis as well as steroid hormone receptors, such as the androgen receptor (AR), which are

*Correspondence to: Phuoc T. Tran; Email: tranp@jhmi.edu
Submitted: 12/12/12; Accepted: 01/15/13
<http://dx.doi.org/10.4161/cbt.23626>

critical for prostate cancer survival.⁹ Targeting Hsp90 is a particularly attractive anticancer and radiosensitizing approach for prostate cancer, as Hsp90 has been reported to be overexpressed in prostate cancer cells as compared to normal prostate epithelium.¹⁰ In addition, Hsp90 inhibition offers a multi-pronged attack on many aberrant pathways critical for prostate tumor maintenance¹¹ and intrinsic radioresistance¹² given the diverse clientele of Hsp90. Apart from the pathways responsible for cell cycle arrest and DNA damage repair, those attributed to radio-protection, such as the PI3K-Akt-mTOR pathway,¹²⁻¹⁴ have protein components that are also stabilized by Hsp90.¹⁵⁻¹⁷

The first class of Hsp90 inhibitors examined were the geldanamycin analogs, specifically 17-allylamino-17-demethoxy-geldanamycin (17-AAG) and 17-(dimethylaminoethylamino)-17-demethoxygeldanamycin (17-DMAG), which have been exhaustively characterized preclinically and have also been tested in several phase I and II clinical trials. The clinical results with these geldanamycin-based agents have been modest. There are several limitations associated with these compounds owing to poor solubility, difficulty in formulation, inconsistent pharmacokinetics, hepatotoxicity, susceptibility to P-glycoprotein efflux and polymorphic metabolism by NQO1/DT-diaphorase enzymes.¹⁸ However, these geldanamycin derivatives have been valuable as a proof of concept, showing that inhibition of Hsp90 has anticancer and radiosensitizing properties in several tumor-derived cell lines in vitro (including prostate, lung, colorectal, glioma and pancreatic carcinomas) and in vivo through tumor xenograft models (human cervical, prostate and head and neck squamous cell carcinoma).¹⁹⁻²⁶

The need to overcome these limitations and improve the efficacy of geldanamycin analogs led to the development of a novel class of Hsp90 inhibitors known as resorcinolytic pyrazoles/isoxazoles that do not possess many of the limitations cited for geldanamycin-based agents. NVP-AUY922 (AUY922), a resorcinol isoxazole, is one of the most potent synthetic small molecule inhibitors of Hsp90.²⁶ Single agent AUY922 has shown potent preclinical anticancer activity in vitro and in vivo against a range of histologic cell types including head and neck squamous cell carcinomas (HNSCC), pancreas, prostate, lung, cervical, colorectal, breast carcinomas, myelomas, melanomas, sarcoma and glioblastoma.²⁶⁻³⁰ A limited number of recent studies have examined AUY922 as a radiosensitizer in vitro. In vivo radiosensitization by AUY922 is limited to a single report examining HNSCC using immunocompromised mice.³¹

In this study we explore the efficacy of AUY922 as a radiosensitizer in both androgen-dependent and AR null prostate cancer cell lines in vitro, as well as demonstrating for the first time potent in vivo radiosensitizing effects of AUY922 on prostate tumors using an immunocompetent model system. We then proceed to investigate plausible mechanisms for AUY922-mediated radiosensitization of prostate cancer cells.

Results

Treatment with AUY922 induced radiosensitization in prostate cancer cell lines in vitro. AUY922 produced a dose-dependent

decrease in critical prostate cancer client proteins and counter-regulatory induction of Hsp72 in prostate cancer cells in vitro (Fig. 1A and B). Members of the PI3K-Akt-mTOR and androgen receptor (AR) pathway (phospho-S6 and the androgen receptor, respectively), counter-regulatory pathways critical for prostate cancer survival,¹¹ were substantially downregulated upon ≥ 50 nM treatment of Myc-CaP cells (Fig. 1A). A similar downregulation of phospho-S6 was observed in the AR null PC3 cells (Fig. 1B). AUY922 has previously been reported to have substantial anticancer activity as a single agent²⁶⁻³⁰ which we confirmed using clonogenic survival assays in vitro. We found that treatment with low nanomolar concentrations of AUY922 reduced the survival fractions impressively to 20% in both Myc-CaP (Fig. 1C, 20 nM) and PC3 (Fig. 1D, 10 nM) cell lines ($p < 0.0001$, Student's t-test). To test the ability of AUY922 to radiosensitize prostate cancer cells in vitro, clonogenic survival assays were again performed with both Myc-CaP (Fig. 1E) and PC3 cells (Fig. 1F). In both cell lines, at both 2 Gy ($p < 0.0001$, Student's t-test) and 4 Gy ($p < 0.0001$, Student's t-test), a substantial decrease in the survival fraction of both cell lines was observed at doses of AUY922 as low as 5–10 nM as compared with vehicle control. The mean AUY922 enhancement ratios were 1.74 (SD 0.2) for Myc-CaP cells and 1.47 (SD 0.11) for PC3 cells.

AUY922 increased radiation-induced apoptosis of prostate cancer cells in vitro. In order to elucidate possible mechanisms that could account for the AUY922-mediated radiosensitization observed in colony formation assays, we examined the degree of apoptosis in prostate cancer cell lines exposed to 24 h incubation with AUY922, then irradiated and media changed after an additional 24 h (48 h total exposure to AUY922). Representative plots of PC3 cells are displayed in Figure 2A and for Myc-CaP cells in Figure 2B, while a summary of the apoptosis assay results are depicted graphically in Figure 2C. The percentages of cells demonstrating an Annexin V (AxV) high/propidium iodide (PI) low staining pattern indicative of early apoptosis (quadrant II) and an AxV high/PI high staining pattern indicative of late apoptosis (quadrant III) were summed to yield the total number of apoptotic cells (Fig. 2C). PC3 cells treated with AUY922 and radiation exhibited a supra-additive increase in proportion of cells undergoing apoptosis (16.92%) compared with cells treated with radiation alone (9.81%; $p = 0.023$, Student's t-test), AUY922 alone (4.95%; $p = 0.001$, Student's t-test) or vehicle control (3.11%; $p = 0.004$, Student's t-test). Notably, treatment with AUY922 alone did not result in a significant increase in apoptosis compared with treatment with vehicle control ($p = 0.19$, Student's t-test). In a similar fashion, a supra-additive increase in proportion of cells undergoing apoptosis was seen among Myc-CaP cells treated with AUY922 and radiation (35.60%) compared with radiation alone (11.58%), AUY922 alone (14.85%) or vehicle control (2.48%; all $p < 0.001$, Student's t-test). In both cell lines, concurrent AUY922 and radiation produced increases in both early and late apoptosis, with the greater absolute increase being in percentage of cells undergoing late apoptosis. Collectively, these data suggest that concurrent treatment with AUY922 and radiation results in a supra-additive increase in apoptotic cell death compared with either therapy alone.

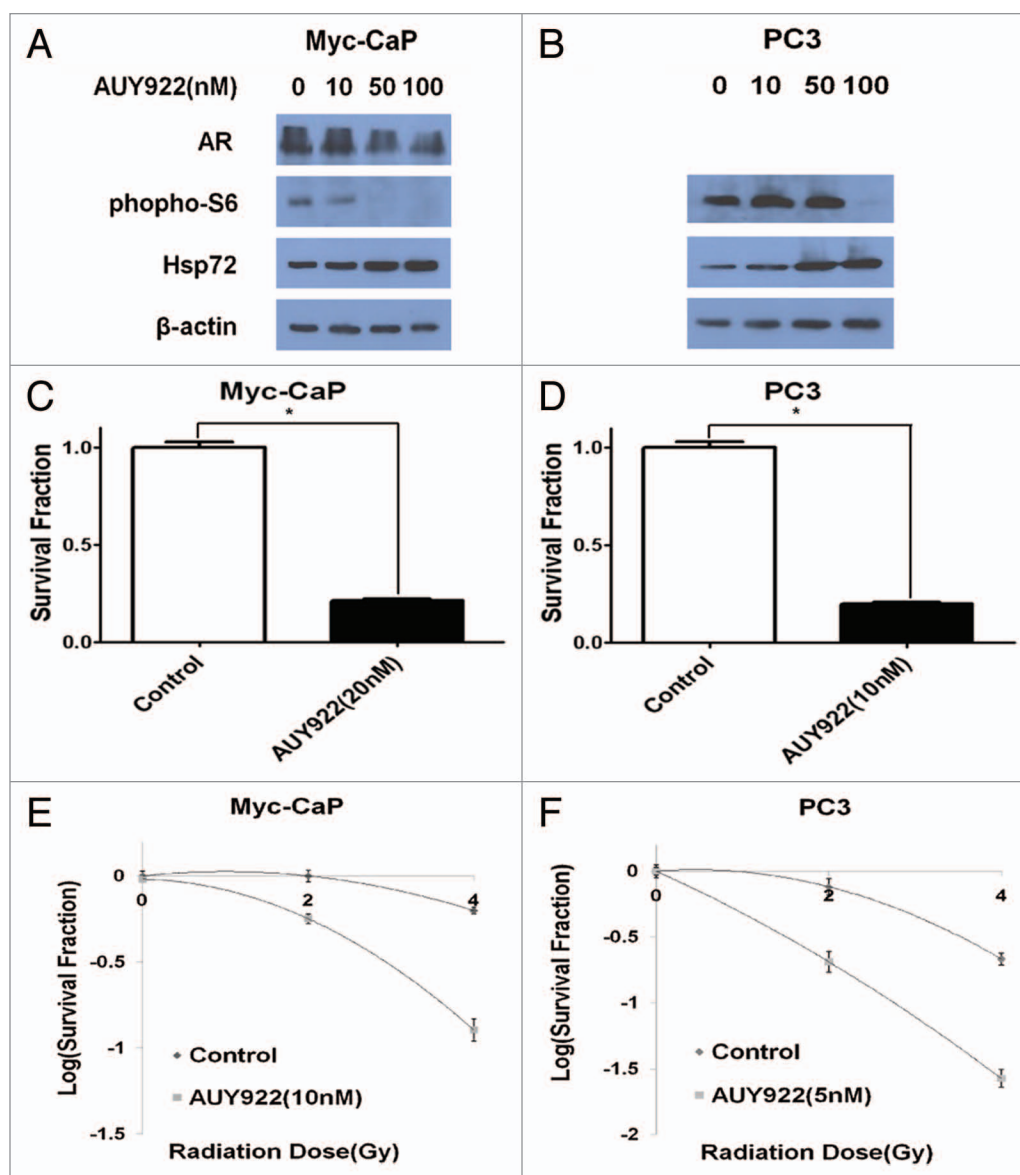


Figure 1. AUY922 radiosensitizes prostate cancer cell lines, Myc-CaP and PC3, in vitro. **(A and B)** Cells were exposed to 24 h of AUY922 at the indicated concentration prior to protein extraction. Western blotting indicated a downregulation of phospho-S6 and androgen receptor (AR), but upregulation of Hsp72 following AUY922 exposure. Clonogenic survival assay depicting the anticancer activity of AUY922 used as a single agent in both **(C)** Myc-CaP and **(D)** PC3 cells ($p < 0.001$). Clonogenic survival assays for **(E)** Myc-CaP and **(F)** PC3 cells demonstrated AUY922-induced radiosensitization in both cell lines with enhancement ratios of 1.74 (SD = 0.2) and 1.47 (SD = 0.11), respectively. All experiments were done in triplicate and repeated at least three times.

AUY922 induced a G_2 -M arrest in prostate cancer cell lines. To further explore mechanisms behind AUY922-induced radiosensitization, treatment effects on the cell cycle of prostate cancer cells were examined (Fig. 3A and B). Attempts to synchronize Myc-CaP cells were unsuccessful, possibly due to the MYC-induced nature of these cells. Therefore, we examined the effects of AUY922 on the cell cycle of unsynchronized Myc-CaP cells (Fig. 3A) and observed that Myc-CaP cells exhibited a higher proportion of cells in G_2 -M following treatment with AUY922. Treatment with vehicle control resulted in 12.5% (SD, 0.9%) of cells in G_2 -M after 24 h, while treatment with 20 nM and 50 nM AUY922 caused 17.6% (SD, 2.2%) and 20.1% (SD, 2.1%) of

cells to be in G_2 -M, respectively (both $p < 0.001$, Student's t-test). Synchronized PC3 cells incubated with AUY922 for 24 h demonstrated an overt G_2 -M arrest, the degree of which increased with higher doses of AUY922 (Fig. 3B). Treatment with AUY922 significantly increased the percentage of cells in G_2 -M from 41.9% (SD 5.5%) after treatment with vehicle control to 65.8% (SD 6.8%) after treatment with 10 nM AUY922 ($p < 0.001$, Student's t-test) and to 82.4% (SD 0.7%) after treatment with 50 nM AUY922 ($p < 0.0001$, Student's t-test). The effect of AUY922 on the Myc-CaP cell cycle was much less pronounced than in PC3 cells, but the same pattern of an increased proportion of cells in G_2 -M after AUY922 treatment was observed. Altogether, these data indicate

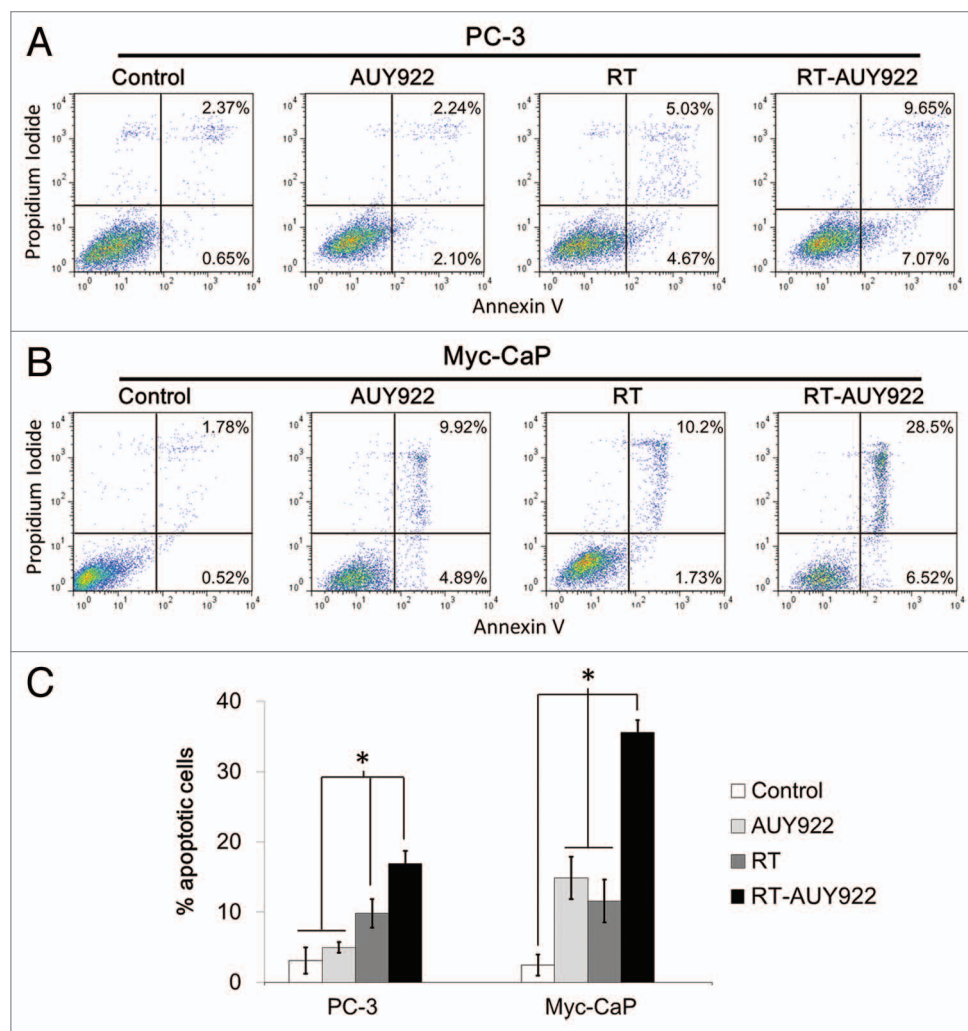


Figure 2. AUY922 given concurrently with radiation (RT) increases the proportion of cells undergoing apoptosis compared with RT alone in vitro. **(A)** PC3 cells were incubated with or without 100 nM AUY922 for 24 h prior to RT and assessed 24 h post-RT for Annexin V-FITC and propidium iodide using flow cytometry. Representative flow cytometry plots for each of the four treatment arms are shown: from left to right, control, AUY922 alone, RT alone and combined RT and AUY922 (RT-AUY922). **(B)** Myc-CaP cells were treated with 100 nM AUY922 and processed for flow cytometry similarly as for PC3 cells above. **(C)** Cells in the early phases of apoptosis (Annexin V high and propidium iodide low) and cells in the late phases of apoptosis (Annexin V high and propidium iodide high) are summed together and plotted as “% apoptotic cells” with SEM for both cell lines. Asterisks represent statistically significant differences between the treatment groups by Student’s t-test (all $p < 0.03$). All experiments were done in triplicate and repeated at least twice.

that AUY922 causes an increase in the proportion of cells in G_2 -M that mechanistically may account for at least part of the radiosensitization observed in our in vitro clonogenic survival assays.

Treatment with AUY922 delayed the repair of radiation induced DNA double stranded breaks. Based on the results obtained from our cell cycle analysis which revealed that AUY922 induced reassortment of prostate cancer cells into more radiosensitive phases of the cell cycle (G_2 -M),³⁵⁻³⁷ we hypothesized these cells may exhibit higher levels of radiation-induced DNA damage. To investigate this hypothesis, we incubated both PC3 and Myc-CaP cells for 24 h with AUY922 (10–20 nM) or vehicle control and then irradiated with 2–4 Gy. Post-irradiation, cells were fixed at time points of < 30 min ($t = 0$ h) as well as later time points of 6 h ($t = 6$ h) for Myc-CaP cells and 24 h ($t = 24$ h) for PC3 cells and subsequently probed for γ -H2AX foci, a marker

for DNA double-strand breaks (DSBs) and counted the number of foci (Fig. 3C–E). When treated with radiation plus AUY922 (RT-AUY922) both prostate cancer cell lines demonstrated a higher proportion of cells with > 25 γ -H2AX foci at $t = 0$ h as compared with the other three arms (Fig. 3D and E, $p < 0.05$ by Fisher’s exact test for all comparisons). At later time points, this pattern was maintained, with a greater proportion of cells treated with RT-AUY922 exhibiting > 25 persistent γ -H2AX foci compared with the other treatment arms (Fig. 3D and E, $p < 0.05$ by Fisher’s exact test for all comparisons). These data suggest that combining AUY922 with RT augments the number of DSBs that are produced and that persist after radiation, possibly due to an increase in the absolute number of DSBs induced and/or delayed DSB repair. We probed by western blotting for AUY922 effects on the DNA damage response (DDR) machinery and observed

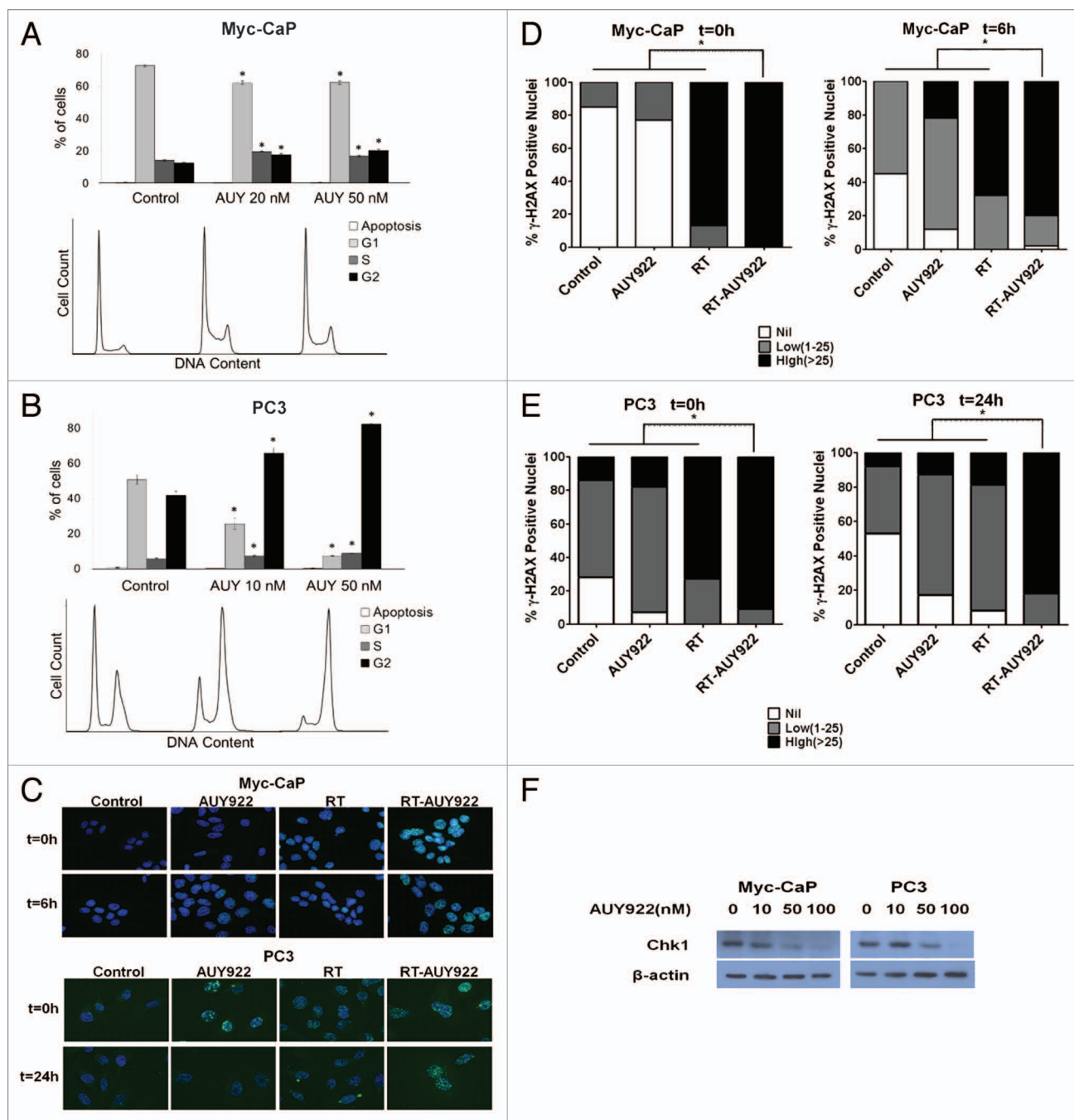


Figure 3. Mechanisms of AUY922 mediated radiosensitization in vitro. **(A)** Unsynchronized Myc-CaP cells were exposed to vehicle control, 20 nM AUY922 or 50 nM AUY922 for 24 h and then fixed with ethanol for cell cycle analysis. **(B)** PC3 cells were synchronized, then re-fed with complete medium (10% serum) either containing vehicle control, 10 nM AUY922 or 50 nM AUY922 for 24 h and then fixed with ethanol for cell cycle analysis. Percent of cells in G₁, S and G₂ phases with SEM is plotted for control and AUY922 arms, with corresponding histograms generated from flow cytometry shown below each bar plot. Treatment with AUY922 caused a G₂-M arrest in unsynchronized Myc-CaP and synchronized PC3 cells at a similar time radiation would be delivered in clonogenic survival experiments in **Figure 1**. Asterisks denote significant differences from corresponding columns in the control arm for each cell line by Student's t-test (all $p < 0.001$). **(C)** Immunofluorescence (IF) for γ -H2AX foci and then staining for DAPI were performed (note: the t = 0 time point actually represents cells that were fixed at < 30 min post-irradiation). Fluorescent images were captured at 63 \times using a fluorescent microscope with uniform exposures of 24 ms for DAPI and 900 ms for Alexa Fluor 488 used for Myc-CaP cells. Images for PC3 cells were taken with uniform exposures of 50 ms for DAPI and 1500 for Alexa Fluor 488. Representative images are shown for the Myc-CaP and PC3 cells at 6h and 24 h respectively, for each of the treatment arms. The percent of nuclei demonstrating high (> 25), moderate (10–25), low (< 10) or no γ -H2AX foci was quantitated for both **(D)** Myc-CaP and **(E)** PC3 cell lines at the time points depicted by counting ≥ 3 representative high-power fields (HPF). The results of this quantitation were represented graphically with SEM for each treatment arm of each cell line **(D and E)**. For both cell lines, radiation and AUY922 (RTAUY922) resulted in a greater percent of nuclei with a high number of γ -H2AX foci at both time points as compared with all of the other arms ($p < 0.05$). Asterisks represent significant differences between treatment arms by Fisher's exact test as indicated by accompanying brackets. All experiments were done in triplicate and repeated. **(F)** Cells were exposed to 24 h of AUY922 at the indicated concentration prior to western blotting for DNA damage response regulator Chk1.

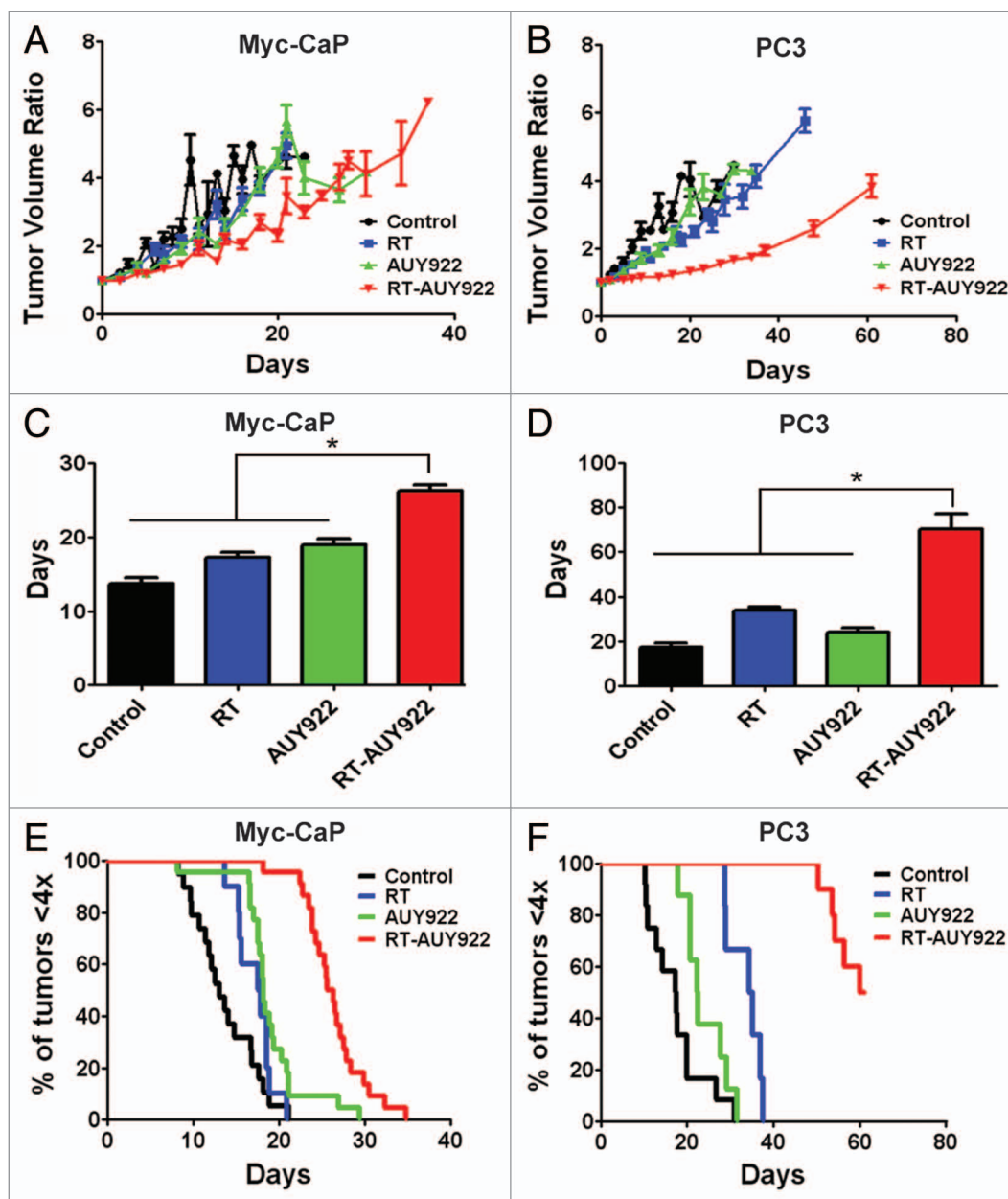


Figure 4. AUY922 radiosensitizes prostate cancer cell lines, Myc-CaP and PC3, in vivo. A hind-flank tumor growth delay model (see Materials and Methods) was used to assay the following treatment arms: (1) no treatment; (2) fractionated radiation 2 Gy \times 3 (RT); (3) AUY922 and (4) AUY922 and RT (RT-AUY922) $n \geq 5$ mice per arm repeated twice in the Myc-CaP model and $n > 3$ mice per arm in PC3 model. The results of the experiment were analyzed using (A and B) fold tumor volume change over time, (C and D) mean time to quadruple the pre-treatment tumor volume and (E and F) Kaplan-Meier survival analysis where the time for quadrupling the pretreatment tumor volume was considered the event of interest. The RT-AUY922 arm was significantly different from any of the other arms using Mann-Whitney U-test and log-rank test for the Myc-CaP model ($p < 0.05$). The same trend was observed in the PC3 model ($p < 0.01$). The AUY922 alone and RT alone arms were significantly different from one another in the PC3 model but not in the Myc-CaP model ($p = 0.0056$ and $p = 0.1123$ by log-rank test, respectively).

that prostate cancer cells exposed to increasing nanomolar levels of AUY922 expressed decreasing levels of the DDR protein Chk1 (Fig. 3F). These results indicate that one mechanism by which AUY922 radiosensitizes prostate cancer cells is through reducing expression of critical components of the DDR machinery required to detect and repair DSBs.

Combined treatment with AUY922 and radiation delayed tumor growth in vivo. We implanted Myc-CaP cells in the hind

flanks of immunocompetent male FVB/N mice and human PC3 cells in athymic nude male mice to assess the effects of AUY922 and fractionated radiation (RT) in vivo (Fig. 4). RT-AUY922 treatment markedly delayed tumor volume quadrupling time in both cell lines compared with the single-treatment and control arms (Fig. 4A and B). In the Myc-CaP tumor hind flank model, the mean tumor quadrupling times were 13.12 d for no treatment, 17.70 d for RT alone, 18.18 d for AUY922 alone and

25.96 d for the combined RT-AUY922 arm (Fig. 4C, $p < 0.0001$ for RT-AUY922 vs. any other arm by Mann-Whitney U-test). Myc-CaP tumors treated with AUY922 and radiation required on average 12.84 d more to quadruple compared with untreated tumors (25.96 d – 13.12 d = 12.84 d). The tumor delay growth observed with combined RT-AUY922 was greater than the sum of increases in Myc-CaP tumor growth delay seen with AUY922 alone and RT alone (4.58 d + 5.06 d = 9.64 d), which suggests that combined RT-AUY922 delays tumor growth in a supra-additive manner. Similarly, using a Kaplan-Meier analysis with an event defined as time to tumor quadrupling, RT-AUY922 resulted in significantly longer median time to quadrupling than either single-treatment arm (Fig. 4E, $p < 0.0001$, log-rank test). The effect of AUY922 in combination with fractionated radiation was even more pronounced in AR-null PC3 hind-flank xenograft tumors, where at the time of experiment termination (61 d total) only 60% of tumors in the RT-AUY922 arm had quadrupled to their pre-treatment volume. The PC3 tumor quadrupling times were 17.38 d for no treatment, 34.80 d for RT, 22.46 d for AUY922 and 60.47 d for RT-AUY922 (Fig. 4D, $p < 0.0001$ for RT-AUY922 vs. the AUY922 and no treatment arms, $p = 0.0002$ vs. RT by Mann-Whitney U-test). These data suggest that RT-AUY922 confers a supra-additive delay in tumor growth on PC3 hind-flank tumors as well. As expected, RT-AUY922 treatment also significantly delayed median time to quadrupling compared with each of the other arms by Kaplan-Meier analysis (Fig. 4F, $p < 0.0001$, log-rank test). For PC3 tumors we also observed that fractionated radiation alone significantly delayed tumor growth compared with AUY922 treatment alone or control (Fig. 4F, $p = 0.0056$ and $p = 0.0007$, respectively, log-rank test). Finally, no observable differences in normal tissue toxicity, such as weight loss, diarrhea, dermatitis and ulceration, were noted between the combined RT-AUY922 arm and either of the single-treatment arms for either Myc-CaP or PC3 tumor engrafted mice. In summary, AUY922 demonstrated potent radiosensitization of both androgen-dependent and AR-null prostate cancer cells in vivo.

Discussion

The results of this study demonstrate the potent ability of the novel Hsp90 inhibitor AUY922 to radiosensitize prostate cancer cells both in vitro and, most importantly, in vivo. We show that AUY922 may radiosensitize prostate cancer cells via multiple mechanisms including, but not limited to, downregulation of the PI3K-Akt-mTOR pathway, reassortment of prostate cancer cells into more radiosensitive phases of the cell cycle through G_2 -M arrest and delay in the repair of radiation-induced DNA DSBs. Our data are consistent with recent studies in other cancer types showing that treatment with AUY922 alone caused cancer cells to arrest at G_2 -M and increased the persistence of radiation-induced DSBs.^{31,35,38} We extend these data by showing that AUY922 can radiosensitize both androgen-dependent and AR-null prostate cancer tumors in vivo and in the setting of an immunocompetent host.

Hsp90 inhibitors can both directly and indirectly modulate expression levels of various client proteins. The PI3K/Akt/mTOR

and AR pathways are two interacting pathways critical for prostate cancer survival and proliferation¹¹ that we show can be downregulated by AUY922 alone. We also observed prominent reduction in clonogenic survival induced by AUY922 treatment alone in both androgen-dependent and AR-null prostate cancer cells (Fig. 1C and D), suggesting that AUY922 may translate well as a single agent for prostate cancer treatment, as has been recently suggested by others.^{26,39}

Targeting Hsp90 with classic geldanamycin inhibitors and more recently with nongeldanamycin based inhibitors, such as AUY922, has demonstrated radiosensitization of cancer cell lines derived from several different histologies.^{19-24,31-35} Hsp90 inhibition offers the theoretical possibility of potent radiosensitization through broad downregulation of multiple critical radioresistance pathways whose components are members of the Hsp90 clientele, such as signal transduction pathways (PI3K-Akt-mTOR)¹²⁻¹⁴ and DNA damage response (DDR) pathways (ATR/Chk1).^{31,38,40} This study suggests that AUY922 may indeed impart radiosensitization through multiple mechanisms: (1) reassortment of prostate cancer cells into G_2 -M, (2) downregulation of the PI3K-Akt-mTOR radioresistance pathway and (3) downregulation of the ATR-Chk1 DDR pathway. Recent studies have shown that the ATR-Chk1 DDR axis is a client pathway of Hsp90 in HeLa and MCF7 cells.³⁸ These findings support the results of our γ -H2AX foci assay (Fig. 3C–E) in which we observed increased production and persistence of radiation-induced DNA DSBs in cells treated with AUY922. Our observations that AUY922 causes a G_2 -M cell cycle arrest and downregulates components of the PI3K-Akt-mTOR pathway are consistent with other studies in non-prostate cancer cell lines.^{32,33}

A key factor for the clinical success of a radiosensitizer is the ability to selectively radiosensitize only tumor cells and not normal tissues. Previous in vitro preclinical studies have demonstrated that geldanamycin Hsp90 inhibitors do not radiosensitize non-cancerous cell lines.^{23,24} These data correspond well to our in vivo findings that no additional normal tissue toxicity was present following combined treatment with AUY922 and fractionated radiation in either immunocompetent or immunocompromised mouse tumor graft models compared with either therapy alone.

The in vivo efficacy of Hsp90 inhibition for radiosensitization has not been extensively characterized. Of the four studies reported, three involved the geldanamycin derivative 17-AAG used in prostate, cervical and HNSCC human tumor xenograft models, while only one study has tested AUY922 (using a HNSCC xenograft model).^{16,21,31,41} Thus, our study shows for the first time that AUY922 mediates potent in vivo radiosensitization of prostate cancer tumors in both immunocompromised and immunocompetent animal models. Combination treatment with a single dose of AUY922 followed by fractionated radiation (RT) increased in a supra-additive fashion the tumor volume quadrupling time as compared with either RT or AUY922 alone. While further mechanistic studies detailing precisely how AUY922 treatment increases the efficacy of radiation in cancer cells are needed, we provide compelling preclinical evidence for AUY922 as a potent radiosensitizer for prostate cancer. AUY922 is currently being tested in several phase I and II trials for advanced

stage colorectal, lung and gastric cancers, but none of these trials include radiation (www.clinicaltrials.gov). Our preclinical findings indicate that AUY922 has promising efficacy as an adjunct to radiation therapy for prostate cancer and clinical studies investigating this therapeutic combination are warranted.

Materials and Methods

Cell lines and cell culture. PC3, a human prostate carcinoma cell line was purchased from the American Type Culture Collection. Myc-CaP cells were prepared from a prostate carcinoma dissected from a Hi-Myc transgenic mouse⁴² and generously provided by Dr John Isaacs (Johns Hopkins Medical Institutions). Both cell lines were checked by short tandem repeat profiling and mycoplasma testing services of the Johns Hopkins Medicine Genetic Resources Core Facility. PC3 cells were grown in F12-K medium supplemented with 10% FBS and 1% penicillin-streptomycin. Myc-CaP cells were grown and maintained in DMEM medium supplemented with 10% FBS and 1% penicillin-streptomycin. All cells were incubated at 37°C in humidified 5% CO₂. Cells were sub-cultured at 70–80% confluence and all experiments were performed with the cells in an exponential growth phase.

Drug treatment. NVP-AUY922 (mesylate) was generously provided by Novartis. The drug was dissolved in DMSO and stored at -20°C in 1 mM aliquots for the in vitro studies. For our in vivo experiments, the drug was formulated in 5% dextrose water and injected at 30 mg/kg by tail vein injection or intraperitoneal injection.

Radiation therapy. For in vitro experiments, cells were irradiated with 0–6 Gy at room temperature using a GammaCell irradiator with a ¹³⁷Cs source at a dose rate of 50 cGy/min. For in vivo experiments, mice were treated using the Small Animal Radiation Research Platform (SARRP).⁴³ The tumors were irradiated with a circular beam of 1 cm diameter.

Clonogenic assay. Cells in exponential growth phase were counted and plated in 10 cm dishes. Depending on the cell type, drug concentration and radiation dose, 150–15,000 cells were plated. Cells were allowed to attach, AUY922 was added to the medium 24 h after plating and then 24 h after AUY922 was added radiation was delivered. The drug was removed 24 h post radiation by freshly adding growth medium and was subsequently replenished every 5–7 d. Colonies were stained and counted 10–14 d after irradiation by fixing with 0.1% Gentian Violet dissolved in a mixture of methanol and DI water in a ratio of 1:1. Colonies were counted under an inverted phase contrast microscope (Nikon Instruments, Inc.) with a colony defined as comprising of at least 50 cells. Surviving fraction was calculated as a function of plating efficiency. All arms were done in triplicates and repeated at least three times.

Cell cycle analysis. For experiments with unsynchronized cells (Myc-CaP), 100,000–300,000 cells were seeded per well in 6-well plates and AUY922 was added 24 h after plating. For experiments with synchronized cells (PC-3), cells were allowed to attach in normal growth media for 24 h, serum starved for 48 h (0% serum), then grown in the presence of 10% serum and aphidicolin (2 µg/mL) for 24 h before being released into normal

growth medium (10% serum) containing AUY922. At various time points, cells were detached, washed with phosphate-buffered saline (PBS) and fixed with chilled 70% ethanol. Cells were pelleted and washed in PBS+1% BSA, then treated with 20 µg/mL RNase-A with 10 µg/mL propidium iodide for 2 h. DNA content was analyzed with a FACSCalibur (BD Biosciences) and FlowJo software (Tree Star).

Apoptosis assay. Apoptosis assays were performed using the FITC Annexin V/Dead Cell Apoptosis Kit with Annexin V-FITC and Propidium Iodide (Invitrogen) for flow cytometry. Cells were seeded at 100,000–300,000 per well in a 6-well plate and treated with 100 nM AUY922 for 24 h prior to irradiation at a dose of 6 Gy (irradiation was omitted in cells treated with AUY922 alone and vehicle control alone). Twenty-four hours post-irradiation, cells were detached, washed in PBS, suspended in binding buffer, and FITC Annexin V (5 µL stock/100 µL buffer) and propidium iodide (100 ng/100 µL buffer) were added. After incubating for 15 min, cells were analyzed with a FACSCalibur (BD Biosciences) and FlowJo software (Tree Star). Unstained and single-stained cells were used to choose the correct gating parameters for each cell line. Experiments were done at least twice in triplicate.

Immunoblot analysis. Cells were plated into 10 cm dishes and grown to sub confluence. AUY922 (1–100 nM) was added to the medium 24 h after plating. Cells were harvested, homogenized 24 h later and 30–50 µg of total protein was loaded into each well of an 8–12% gel and separated. Protein was transferred onto a polyvinylidene fluoride (BioRad) blotting membrane and blocked for an hour using 5% BSA in TBST (Tris-buffered Saline supplemented with 0.1% Tween 20). Phospho-antibodies were incubated with 5% BSA in TBST; other antibodies were incubated with 5% milk in TBST. The membranes were probed with antibodies for phospho-S6, Chk1 (Santa Cruz), androgen receptor (AR) (Santa Cruz), HSP72 (Selleck chemicals) and subsequently with horseradish peroxidase-labeled mouse anti-rabbit secondary antibodies (Sigma-Aldrich). Each antibody incubation step was followed by 3–4 washes with TBST. The secondary antibody was then coupled with GE ECL Plus kit (GE Life Sciences) and protein levels were detected using autoradiography films (Denville Scientific, Inc.). Experiments were done at least twice.

Immunofluorescence. Cells were plated on poly-L-lysine-coated (13.3 mg/ml) glass chamber slides/ cover glass and incubated for 24 h at 37°C in 5% CO₂ and fixed for 15 min with freshly prepared 4% paraformaldehyde in phosphate-buffered saline (PBS). After washing with PBS, the cells were permeabilized for 15 min with PBST (PBS with 0.1% Triton X-100). The cells were then blocked with 2% FBS, 3% BSA (bovine serum albumin) in PBS for 30 min and incubated at room temperature for 1 h with primary antibody (1:250) diluted in PBS. After washing with PBS, the cells were incubated with an Alexa Fluor 488-conjugated secondary antibody (1:300, Molecular Probes) for one h at room temperature. Cells were washed in PBS and coverslips stained with DAPI prior to mounting. Fluorescent images were captured using a fluorescent confocal microscope. The cells were probed with primary antibodies for γH2AX (Millipore).

Mouse tumor graft models and tumor growth delay experiments. Eight-week-old male FVB/N mice were purchased from Taconic (Taconic Farms Inc.). Mice were maintained under pathogen-free conditions and given food and water ad libitum in accordance with guidelines from the Johns Hopkins Animal Care and Use Committee. Mice were injected subcutaneously in both flanks with 1×10^6 Myc-CaP cells in 100 μ L of Hanks and Matrigel (Invitrogen) mixed in 1:1 ratio. Once tumors reached 100 mm³, 5–6 mice were randomly assigned to each of the four treatment arms: (1) no treatment, (2) AUY922 only, (3) radiation only and (4) AUY922 + radiation (RT-AUY922). Mice in AUY922 treated arms were given a single dose of 30 mg/kg, intravenously through the tail vein on the first day of treatment. The radiation arms were irradiated according to a fractionated scheme wherein, the mice were radiated for three consecutive days with a 2 Gy focal beam. Mice allocated to the combination arm were also subjected to the same fractionated radiation scheme as the radiation alone arm, with the first fraction of radiation being delivered 6 h post drug treatment. The tumors were measured three times a week, until the tumors reached four times (4 \times) their pre-treatment volume. Tumor volume was calculated using the formula: length \times width \times height $\times \pi/6$. The androgen receptor null PC3 xenograft experiments were performed on 6–8-week-old athymic male nude mice (Harlan, Inc.). The mice were injected subcutaneously in both flanks with 1.5×10^6 cells, in 100 μ L of PBS and Matrigel (Invitrogen) mixed in 1:1 ratio, following the same protocol and treatment scheme as mentioned above, except for that AUY922 was administered intraperitoneally. All experiments repeated twice.

Statistics. Error bars included in graphical figures represent standard error of the mean (SEM). Two-tailed unpaired Student's t-test was used to compare apoptosis assay and cell cycle

analysis between treatment arms. Fisher's exact test was used to compare γ -H2AX foci analysis results between treatment arms. Clonogenic survival curves were fitted with a linear quadratic model using SPSS Statistics version 19 using a least squares fit, weighted to minimize the relative distances squared and compared using the extra-sum of squares F-test. Mean inactivation doses were determined using the method of Fertl⁴⁴ and enhancement ratios calculated as the ratio of the mean inactivation dose for control vs. AUY922-treated arms as described by Morgan.⁴⁵ A value significantly > 1 indicates radiosensitization. Tumor growth delay assay results were compared by two distinct methods: (1) by using the log rank test to compare median quadrupling times after creating a Kaplan-Meier plot using quadrupling in volume as the event of interest and (2) by comparing quadrupling times between all tumors in two arms using the Mann-Whitney U-test. A two-sided α value of ≤ 0.05 was considered significant in all cases.

Disclosure of Potential Conflicts of Interest

The authors have no conflicts of interest to disclose.

Acknowledgments

We thank members of the Tran, Bunz and DeWeese laboratories for helpful discussions and/or a critical reading of the manuscript. A.T.W. was funded by an RSNA research medical student grant. R.D.W. was a Johns Hopkins Laboratory Radiation Oncology Training Fellow (NIH-T32CA121937). P.T.T. was funded by the Phyllis and Brian L. Harvey Scholar Award from the Patrick C. Walsh Prostate Cancer Research Fund, a DoD Prostate Cancer Physician Research Training Award (W81XWH-11-1-0272), an ACS Scholar award (122688-RSG-12196-01-TBG) and the NIH (P30CA006973).

References

1. Siegel R, Naishadham D, Jemal A. Cancer statistics, 2012. *CA Cancer J Clin* 2012; 62:10-29; PMID:22237781; <http://dx.doi.org/10.3322/caac.20138>.
2. Mohler JL, Armstrong AJ, Bahnson RR, Boston B, Busby JE, D'Amico AV, et al. Prostate cancer, Version 3.2012: featured updates to the NCCN guidelines. *J Natl Compr Canc Netw* 2012; 10:1081-7; PMID:22956807.
3. Sandler HM, Mirhadi AJ. Radical radiotherapy for prostate cancer is the 'only way to go'. [Williston Park]. *Oncology (Williston Park)* 2009; 23:840-3; PMID:19839425.
4. Jones CU, Hunt D, McGowan DG, Amin MB, Chetner MP, Bruner DW, et al. Radiotherapy and short-term androgen deprivation for localized prostate cancer. *N Engl J Med* 2011; 365:107-18; PMID:21751904; <http://dx.doi.org/10.1056/NEJMoa1012348>.
5. Horwitz EM, Bae K, Hanks GE, Porter A, Grignon DJ, Brereton HD, et al. Ten-year follow-up of radiation therapy oncology group protocol 92-02: a phase III trial of the duration of elective androgen deprivation in locally advanced prostate cancer. *J Clin Oncol* 2008; 26:2497-504; PMID:18413638; <http://dx.doi.org/10.1200/JCO.2007.14.9021>.
6. Bannuru RR, Dvorak T, Obadan N, Yu WW, Patel K, Chung M, et al. Comparative evaluation of radiation treatments for clinically localized prostate cancer: an updated systematic review. *Ann Intern Med* 2011; 155:171-8; PMID:21646550.
7. Luo J, Solimini NL, Elledge SJ. Principles of cancer therapy: oncogene and non-oncogene addiction. *Cell* 2009; 136:823-37; PMID:19269363; <http://dx.doi.org/10.1016/j.cell.2009.02.024>.
8. Pearl LH, Prodromou C. Structure and in vivo function of Hsp90. *Curr Opin Struct Biol* 2000; 10:46-51; PMID:10679459; [http://dx.doi.org/10.1016/S0959-440X\(99\)00047-0](http://dx.doi.org/10.1016/S0959-440X(99)00047-0).
9. Pratt WB. The hsp90-based chaperone system: involvement in signal transduction from a variety of hormone and growth factor receptors. *Proc Soc Exp Biol Med* 1998; 217:420-34; PMID:9521088.
10. Cardillo MR, Ippoliti F. IL-6, IL-10 and HSP-90 expression in tissue microarrays from human prostate cancer assessed by computer-assisted image analysis. *Anticancer Res* 2006; 26(5A):3409-16; PMID:17094460.
11. Carver BS, Chapinski C, Wongvipat J, Hieronymus H, Chen Y, Chandralapaty S, et al. Reciprocal feedback regulation of PI3K and androgen receptor signaling in PTEN-deficient prostate cancer. *Cancer Cell* 2011; 19:575-86; PMID:21575859; <http://dx.doi.org/10.1016/j.ccr.2011.04.008>.
12. Fraser M, Harding SM, Zhao H, Coackley C, Durocher D, Bristow RG. MRE11 promotes AKT phosphorylation in direct response to DNA double-strand breaks. *Cell Cycle* 2011; 10:2218-32; PMID:21623170; <http://dx.doi.org/10.4161/cc.10.13.16305>.
13. Bozulic L, Surucu B, Hynx D, Hemmings BA. PKBalpha/Akt1 acts downstream of DNA-PK in the DNA double-strand break response and promotes survival. *Mol Cell* 2008; 30:203-13; PMID:18439899; <http://dx.doi.org/10.1016/j.molcel.2008.02.024>.
14. Surucu B, Bozulic L, Hynx D, Parcellier A, Hemmings BA. In vivo analysis of protein kinase B (PKB)/Akt regulation in DNA-PKcs-null mice reveals a role for PKB/Akt in DNA damage response and tumorigenesis. *J Biol Chem* 2008; 283:30025-33; PMID:18757368; <http://dx.doi.org/10.1074/jbc.M803053200>.
15. Schulte TW, Blagosklonny MV, Ingui C, Neckers L. Disruption of the Raf-1-Hsp90 molecular complex results in destabilization of Raf-1 and loss of Raf-1-Ras association. *J Biol Chem* 1995; 270:24585-8; PMID:7592678; <http://dx.doi.org/10.1074/jbc.270.41.24585>.
16. Bull EE, Dote H, Brady KJ, Burgan WE, Carter DJ, Cerra MA, et al. Enhanced tumor cell radiosensitivity and abrogation of G2 and S phase arrest by the Hsp90 inhibitor 17-(dimethylaminoethylamino)-17-demethoxygeldanamycin. *Clin Cancer Res* 2004; 10:8077-84; PMID:15585643; <http://dx.doi.org/10.1158/1078-0432.CCR-04-1212>.
17. Camphausen K, Tofilon PJ. Inhibition of Hsp90: a multitarget approach to radiosensitization. *Clin Cancer Res* 2007; 13:4326-30; PMID:17671112; <http://dx.doi.org/10.1158/1078-0432.CCR-07-0632>.
18. Kelland LR, Sharp SY, Rogers PM, Myers TG, Workman P. DT-Diaphorase expression and tumor cell sensitivity to 17-allylamino, 17-demethoxygeldanamycin, an inhibitor of heat shock protein 90. *J Natl Cancer Inst* 1999; 91:1940-9; PMID:10564678; <http://dx.doi.org/10.1093/jnci/91.22.1940>.

19. Russell JS, Burgan W, Oswald KA, Camphausen K, Tofilon PJ. Enhanced cell killing induced by the combination of radiation and the heat shock protein 90 inhibitor 17-allylamino-17-demethoxygeldanamycin: a multitarget approach to radiosensitization. *Clin Cancer Res* 2003; 9:3749-55; PMID:14506167.
20. Dote H, Cerna D, Burgan WE, Camphausen K, Tofilon PJ. ErbB3 expression predicts tumor cell radiosensitization induced by Hsp90 inhibition. *Cancer Res* 2005; 65:6967-75; PMID:16061682; <http://dx.doi.org/10.1158/0008-5472.CAN-05-1304>.
21. Yin X, Zhang H, Lundgren K, Wilson L, Burrows F, Shores CG. BIB021, a novel Hsp90 inhibitor, sensitizes head and neck squamous cell carcinoma to radiotherapy. *Int J Cancer* 2010; 126:1216-25; PMID:19662650.
22. Machida H, Nakajima S, Shikano N, Nishio J, Okada S, Asayama M, et al. Heat shock protein 90 inhibitor 17-allylamino-17-demethoxygeldanamycin potentiates the radiation response of tumor cells grown as monolayer cultures and spheroids by inducing apoptosis. *Cancer Sci* 2005; 96:911-7; PMID:16367912; <http://dx.doi.org/10.1111/j.1349-7006.2005.00125.x>.
23. Machida H, Matsumoto Y, Shirai M, Kubota N. Geldanamycin, an inhibitor of Hsp90, sensitizes human tumour cells to radiation. *Int J Radiat Biol* 2003; 79:973-80; PMID:14713575; <http://dx.doi.org/10.1080/09553000310001626135>.
24. Matsumoto Y, Machida H, Kubota N. Preferential sensitization of tumor cells to radiation by heat shock protein 90 inhibitor geldanamycin. *J Radiat Res* 2005; 46:215-21; PMID:15988140; <http://dx.doi.org/10.1269/jrr.46.215>.
25. Moran DM, Gawlak G, Jayaprakash MS, Mayar S, Maki CG. Geldanamycin promotes premature mitotic entry and micronucleation in irradiated p53/p21 deficient colon carcinoma cells. *Oncogene* 2008; 27:5567-77; PMID:18504430; <http://dx.doi.org/10.1038/onc.2008.172>.
26. Eccles SA, Massey A, Raynaud FI, Sharp SY, Box G, Valenti M, et al. NVP-AUY922: a novel heat shock protein 90 inhibitor active against xenograft tumor growth, angiogenesis, and metastasis. *Cancer Res* 2008; 68:2850-60; PMID:18413753; <http://dx.doi.org/10.1158/0008-5472.CAN-07-5256>.
27. Jensen MR, Schoepfer J, Radimerski T, Massey A, Guy CT, Brueggen J, et al. NVP-AUY922: a small molecule HSP90 inhibitor with potent antitumor activity in pre-clinical breast cancer models. *Breast Cancer Res* 2008; 10:R33; PMID:18430202; <http://dx.doi.org/10.1186/bcr1996>.
28. Moser C, Lang SA, Hackl C, Wagner C, Scheiffert E, Schlitt HJ, et al. Targeting HSP90 by the novel inhibitor NVP-AUY922 reduces growth and angiogenesis of pancreatic cancer. *Anticancer Res* 2012; 32:2551-61; PMID:22753713.
29. Chatterjee M, Andrulis M, Stühmer T, Müller E, Hofmann C, Steinbrunn T, et al. The PI3K/Akt signalling pathway regulates the expression of Hsp70, which critically contributes to Hsp90-chaperone function and tumor cell survival in multiple myeloma. *Haematologica* 2012; PMID:23065523.
30. Ueno T, Tsukuda K, Toyooka S, Ando M, Takaoka M, Soh J, et al. Strong anti-tumor effect of NVP-AUY922, a novel Hsp90 inhibitor, on non-small cell lung cancer. *Lung Cancer* 2012; 76:26-31; PMID:21996088; <http://dx.doi.org/10.1016/j.lungcan.2011.09.011>.
31. Zaidi S, McLaughlin M, Bhide SA, Eccles SA, Workman P, Nutting CM, et al. The HSP90 inhibitor NVP-AUY922 radiosensitizes by abrogation of homologous recombination resulting in mitotic entry with unresolved DNA damage. *PLoS One* 2012; 7:e35436; PMID:22523597; <http://dx.doi.org/10.1371/journal.pone.0035436>.
32. Niewidok N, Wack LJ, Schiessl S, Stingl L, Katzer A, Polat B, et al. Hsp90 Inhibitors NVP-AUY922 and NVP-BEP800 May Exert a Significant Radiosensitization on Tumor Cells along with a Cell Type-Specific Cytotoxicity. *Transl Oncol* 2012; 5:356-69; PMID:23066444.
33. Stingl L, Niewidok N, Müller N, Selle M, Djuzenova CS, Flentje M. Radiosensitizing effect of the novel Hsp90 inhibitor NVP-AUY922 in human tumour cell lines silenced for Hsp90α. *Strahlenther Onkol* 2012; 188:507-15; PMID:22441439; <http://dx.doi.org/10.1007/s00066-012-0080-9>.
34. Schilling D, Bayer C, Li W, Molls M, Vaupel P, Multhoff G. Radiosensitization of normoxic and hypoxic h1339 lung tumor cells by heat shock protein 90 inhibition is independent of hypoxia inducible factor-1α. *PLoS One* 2012; 7:e31110; PMID:22347438; <http://dx.doi.org/10.1371/journal.pone.0031110>.
35. Stingl L, Stühmer T, Chatterjee M, Jensen MR, Flentje M, Djuzenova CS. Novel HSP90 inhibitors, NVP-AUY922 and NVP-BEP800, radiosensitize tumour cells through cell-cycle impairment, increased DNA damage and repair protraction. *Br J Cancer* 2010; 102:1578-91; PMID:20502461; <http://dx.doi.org/10.1038/sj.bjc.6605683>.
36. Terasima T, Tolmach LJ. Changes in x-ray sensitivity of HeLa cells during the division cycle. *Nature* 1961; 190:1210-1; PMID:13775960; <http://dx.doi.org/10.1038/1901210a0>.
37. Biade S, Stobbe CC, Chapman JD. The intrinsic radiosensitivity of some human tumor cells throughout their cell cycles. *Radiat Res* 1997; 147:416-21; PMID:9092920; <http://dx.doi.org/10.2307/3579497>.
38. Ha K, Fiskus W, Rao R, Balusu R, Venkannagari S, Nalabothula NR, et al. Hsp90 inhibitor-mediated disruption of chaperone association of ATR with hsp90 sensitizes cancer cells to DNA damage. *Mol Cancer Ther* 2011; 10:1194-206; PMID:21566061; <http://dx.doi.org/10.1158/1535-7163.MCT-11-0094>.
39. Centenera MM, Gillis JL, Hanson AR, Jindal S, Taylor RA, Risbridger GP, et al. Australian Prostate Cancer BioResource. Evidence for efficacy of new Hsp90 inhibitors revealed by ex vivo culture of human prostate tumors. *Clin Cancer Res* 2012; 18:3562-70; PMID:22573351; <http://dx.doi.org/10.1158/1078-0432.CCR-12-0782>.
40. Wang X, Ma Z, Xiao Z, Liu H, Dou Z, Feng X, et al. Chk1 knockdown confers radiosensitization in prostate cancer stem cells. *Oncol Rep* 2012; 28:2247-54; PMID:23027394.
41. Bisht KS, Bradbury CM, Mattson D, Kaushal A, Sowers A, Markovina S, et al. Geldanamycin and 17-allylamino-17-demethoxygeldanamycin potentiate the in vitro and in vivo radiation response of cervical tumor cells via the heat shock protein 90-mediated intracellular signaling and cytotoxicity. *Cancer Res* 2003; 63:8984-95; PMID:14695217.
42. Watson PA, Ellwood-Yen K, King JC, Wongvipat J, Lebeau MM, Sawyers CL. Context-dependent hormone-refractory progression revealed through characterization of a novel murine prostate cancer cell line. *Cancer Res* 2005; 65:11565-71; PMID:16357166; <http://dx.doi.org/10.1158/0008-5472.CAN-05-3441>.
43. Wong J, Armour E, Kazanzides P, Iordachita I, Tryggstad E, Deng H, et al. High-resolution, small animal radiation research platform with x-ray tomographic guidance capabilities. *Int J Radiat Oncol Biol Phys* 2008; 71:1591-9; PMID:18640502; <http://dx.doi.org/10.1016/j.ijrobp.2008.04.025>.
44. Fertl B, Dertinger H, Courdi A, Malaise EP. Mean inactivation dose: a useful concept for intercomparison of human cell survival curves. *Radiat Res* 1984; 99:73-84; PMID:6739728; <http://dx.doi.org/10.2307/3576448>.
45. Morgan MA, Parsels LA, Kollar LE, Normolle DP, Maybaum J, Lawrence TS. The combination of epidermal growth factor receptor inhibitors with gemcitabine and radiation in pancreatic cancer. *Clin Cancer Res* 2008; 14:5142-9; PMID:18698032; <http://dx.doi.org/10.1158/1078-0432.CCR-07-4072>.